good. A very high number of equidistant meridional streaks are observed, together with broad equatorial and smeared out (*hkl*) reflections. The most prominent equatorial reflections have *d* spacings of 3.56 and 5.93 Å, which are interpreted in terms of the perpendicular and center-to-center separation of adjacent molecules.

The repeat unit length in c-bisthiazole is 12.35 Å, as measured by the C(14) to C(21) separation. Although polymer possessing this heteroatom disposition has not been prepared to date, the crystallographic analysis of the c-bisthiazole model compound implies that individual chains of such material, if synthesized, would adopt an all-planar conformation. Intramolecular steric effects appear to be minimal, and the relative orientation of ring moieties within a particular chain seems to be dominated by resonance and lattice energy terms.

**Supplementary Material Available:** Thermal parameters and structure factor tables for 2,6-diphenylbenzo[1,2-*d*:4,5-*d*']-bisthiazole and 2,6-diphenylbenzo[1,2-*d*:5,4-*d*']bisthiazole (51 pages). Ordering information is given on any current masthead page.

## References and Notes


(1) Helminiak, T. E. *Prepr., Am. Chem. Soc., Div. Org. Coat. Plast.* **1979**, *40*, 475.
(2) Thomas, E. L.; Farris, R. J.; Hsu, S. L. Technical Report AF-WAL-TR-80-4045, 1980.
(3) Welsh, W. J.; Bhaumik, D.; Mark, J. E. *Macromolecules*, this issue.
(4) Wolfe, J. F.; Loo, B. H.; Arnold, F. E. *Macromolecules*, this issue.
(5) Miller, P. T.; Lenhert, P. G.; Joesten, M. D. *Inorg. Chem.* **1972**, *11*, 2221.
(6) Wehe, D. J.; Busing, W. R.; Levy, H. A. "ORABS", Report ORNL-TM-229, Oak Ridge National Laboratory: Oak Ridge, Tenn., 1962.
(7) Stewart, J. F.; Kundell, F. A.; Baldwin, J. C. "X-ray System", Report TR-192, Computer Science Center, University of Maryland: College Park, Md., June 1972.
(8) Cromer, D. T.; Mann, J. B. *Acta Crystallogr., Sect. A* **1968**, *24*, 321.
(9) Stewart, R. F.; Davidson, E. R.; Simpson, W. T. *J. Chem. Phys.* **1965**, *42*, 3175.
(10) Trus, B. L.; Marsh, R. E. *Acta Crystallogr., Sect. B* **1973**, *29*, 2298.
(11) Form, G. R.; Raper, E. S.; Downie, T. C. *Acta Crystallogr., Sect. B* **1974**, *30*, 342.
(12) Bart, J. C. J.; Bassi, I. W.; Benedicenti, C.; Calcaterra, M.; Intrito, R. *Acta Crystallogr., Sect. B* **1978**, *34*, 3639.
(13) Destro, R. *Acta Crystallogr., Sect. B* **1978**, *34*, 959.
(14) Matthews, B. W. *Acta Crystallogr.* **1964**, *17*, 1413.
(15) Dance, I. G.; Isaac, D. *Aust. J. Chem.* **1977**, *30*, 2425.
(16) Ekstrand, J. D.; van der Helm, D. *Acta Crystallogr., Sect. B* **1977**, *33*, 1012.
(17) Adams, W. W.; Azâroff, L. V.; Kulshreshtha, A. K. *Z. Kristallogr.* **1979**, *150*, 321.
(18) Roche, E. J.; Takahashi, T.; Thomas, E. L. *ACS Symp. Ser.* **1980**, *No. 141*, 303.
(19) Atkins, E. D. T.; Keller, A.; Odell, J. A., submitted for publication.


# Rheological Properties of Rodlike Polymers in Solution. 1. Linear and Nonlinear Steady-State Behavior

**S.-G. Chu, S. Venkatraman, G. C. Berry,* and Y. Einaga**

*Department of Chemistry, Carnegie-Mellon University, Pittsburgh, Pennsylvania 15213.*
*Received December 8, 1980*

ABSTRACT: Steady-state rheological properties are reported for solutions of three mesogenic rodlike polymers. Concentrations $c$ range from 0.02 to 0.15 g/mL, depending on the chain length $L$ of the polymer studied, with all solutions being isotropic. The data include the viscosity $\eta_\kappa$ and recoverable compliance $R_\kappa$ determined as a function of shear rate $\kappa$, using a cone-and-plate rheometer, and their limiting values $\eta_0$ and $R_0$, respectively, at small $\kappa$. Rheooptical studies are also reported, giving the birefringence $\Delta n_{13}$ as a function of $\kappa$. The dependence of $\eta_0$ and $R_0$ on concentration and chain length is compared with theoretical predictions. The rapid increase of $\eta_0/M[\eta]$ with increasing $cL$ predicted theoretically is observed (with $M$ the molecular weight and $[\eta]$ the intrinsic viscosity). Behavior attributed to intermolecular association is described for some of the solutions. The nonlinear rheological and rheooptical data show that $\eta_\kappa/\eta_0$, $R_\kappa/R_0$, and $\Delta n_{13}/c$ can be expressed as superposed functions of the reduced strain rate $\tau_c\kappa$ over the range of $c$, $M$, and temperature studied, where $\tau_c$ is equal to $\eta_0 R_0$. The dependence of $\eta_\kappa/\eta_0$ on $\tau_c\kappa$ found for the solutions of rodlike polymers is similar to that observed for flexible chains; a theoretical model for rodlike chains gives qualitatively similar behavior.

Rheological properties of three polymers with rodlike conformations will be described in a series of papers. The first two of this series will deal with certain steady-state rheological properties of isotropic solutions and optically anisotropic solutions. Later papers will concern transient rheological properties of these same materials. The polymers used in this study include poly(*p*-phenylene-2,6-benzobisthiazole) and poly(*p*-phenylene-2,6-benzobisoxazole) with the repeating units

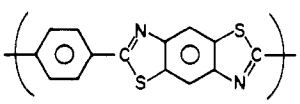

PBT

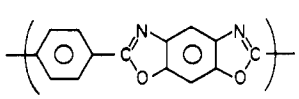

PBO

and poly(*p*-phenyleneterephthalamide) with repeating unit

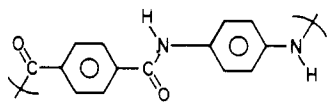

PPTA

Both PBT and PBO have rodlike conformations, characterized by a persistence length $\rho$ that is comparable with or larger than the contour length $L$, and for the PPTA molecules studied here the ratio $\rho/L$ is of order unity. Thus, all three polymers can be expected to exhibit the properties of rodlike molecules. Indeed, all three will form

0024-9297/81/2214-0939$01.25/0 

nematic liquid crystalline solutions under appropriate conditions. Calculations of Flory et al.[1] predict that the volume fraction $\varphi$ of polymer required for thermodynamic stability of the nematic state for an athermal solution is approximately given by

$$\varphi_c = Ad/L \tag{1}$$

where $A$ depends on the polydispersity (e.g., for large $L/d$, $A$ is 8 for a monodisperse polymer and 1 for polymer with a most-probable distribution) and $L$ and $d$ are the length and diameter, respectively, of the rodlike chain.

The properties to be considered here include the limiting values at low shear rate of the viscosity $\eta_0$, the linear steady-state recoverable compliance $R_0$ (often denoted $J_e^\circ$), and the intrinsic birefringence $\Delta n_\infty$. In addition to these parameters, we will also be interested in the following functions, involving ratios of steady-state properties at rate of strain $\kappa$ divided by an appropriate limiting value:

$$\eta_\kappa/\eta_0 = Q(\tau_c\kappa) \tag{2}$$

$$R_\kappa/R_0 = P(\tau_c\kappa) \tag{3}$$

$$\Delta n/\Delta n_\infty = M(\tau_c\kappa) \tag{4}$$

Here, $\eta_\kappa$ is the ratio $\sigma/\kappa$ of the shear stress $\sigma$ to the shear rate $\kappa$ measured in steady-state flow, $R_\kappa$ is the ratio $\gamma_R/\eta_\kappa\kappa$ of the ultimate recoverable strain $\gamma_R$ following cessation of steady-state flow to the stress imposed during the flow, and $\Delta n$ is the difference in the principal components of the refractive index ellipsoid of the solution; $\Delta n$ increases from 0 to $\Delta n_\infty$ as $\tau_c\kappa$ increases from zero. The characteristic time $\tau_c$ is given by

$$\tau_c = \eta_0 R_0 \tag{5}$$

With the systems studied in this part, it is possible to determine each of the limiting parameters $\eta_0$ and $R_0$, so that the functions $Q$ and $P$ in eq 2 and 3 are well-defined. For solutions with $\varphi$ about equal to or larger than $\varphi_c$, this is not always possible.

Although we will not report data on the first normal stress difference $N_\kappa^{(1)}$, it will be convenient to refer to the function

$$S_\kappa = N_\kappa^{(1)}/2(\eta_\kappa\kappa)^2 \tag{6}$$

and its limiting values $S_0$ at small $\kappa$ and to define the ratio

$$S_\kappa/S_0 = N(\tau_c\kappa) \tag{7}$$

Of course, for simple fluids,[2] $S_0 = R_0$. On the other hand, there is no reason to believe that $P$ and $N$ are equal for all $\tau_c\kappa$; see below.

In eq 2, 3, and 7, $Q$, $P$, and $N$ have been written as explicit functions of the reduced shear rate $\tau_c\kappa$. Experimental studies on solutions of flexible-chain polymers[3] and theoretical studies[4] have shown that $\tau_c\kappa$ is a useful and natural variable to use in expressing the dependence of $Q$, $P$, and $N$ on $\kappa$. For example, for many materials, the functions so defined are independent of temperature. In addition, it has been found that for a given solute, $Q$ and $P$ are often nearly independent of $\varphi$ over a wide range. Of course, deviation from this behavior must be expected for large $\tau_c\kappa$, in the so-called "upper Newtonian" range, for which, for example, $Q$ exhibits a plateau value that depends on $\varphi$. For flexible-chain polymers, $Q$ is unity for small $\tau_c\kappa$ and crosses over to a decreasing function of $\tau_c\kappa$ for $\tau_c\kappa$ in the range of unity. Similarly, $P$ is unity for small $\tau_c\kappa$, but the behavior for large $\tau_c\kappa$ is less easily summarized. Typically, with increasing $\kappa$, $P$ decreases from its limiting value for very small $\tau_c\kappa$ for polymers with a broad distribution of molecular weight but may depend only weakly on $\tau_c\kappa$ for polymers with a narrow molecular weight distribution.

The function $M$ depends on the distribution of molecular orientations with the flow direction, and the usual relations are based on an assumed coincidence of the principal directions of the stress and refractive index ellipsoids; this approximation is termed the stress-optical law. Thus, for shear flow, the difference $\Delta p$ of the two principal stresses in the flow plane is related to the shear stress $\eta_\kappa\kappa$ and the first normal stress difference $N_\kappa^{(1)}$ by the expressions (see, for example, ref 5, section 1.2)

$$\Delta p \sin 2\chi' = 2\eta_\kappa\kappa \tag{8}$$

$$\cot 2\chi' = S_\kappa\eta_\kappa\kappa \tag{9}$$

where $\chi'$ is the angle between the flow direction and a principal stress axis in the flow plane (chosen so that $\chi' \leq \pi/4$). The stress-optical law assumes that

$$\Delta n/\Delta p = C \tag{10a}$$

$$\chi = \chi' \tag{10b}$$

where $\chi$ is the extinction angle locating the cross of isocline (i.e., the locus of minimum intensity in the flow plane) defining the angle in the flow plane between the flow direction and a principal axis of the refractive index ellipsoid ($\chi \leq \pi/4$). Coleman and co-workers[6] have demonstrated that these relations are expected to apply for simple fluids in the limit of what are termed "slow flows", for which the limiting relations at small $\tau_c\kappa$ obtain:

$$\Delta n = 2C\eta_0\kappa/\sin 2\chi \tag{11}$$

$$\cot 2\chi = S_0\eta_0\kappa \tag{12}$$

They also find that the stress-optical law cannot be generally assumed for larger $\tau_c\kappa$. Nonetheless, experience has frequently shown that eq 11 and 12 can be used with constant $C$ even for $\tau_c\kappa$ large enough that $Q \leq 1$, if modified by substitution of $\eta_0$ and $S_0$ by $\eta_\kappa$ and $S_\kappa$, respectively (e.g., examples cited in section 1.4 of ref 5). Equations 11 and 12 so modified give $\Delta n$ implicitly as a function of $\tau_c\kappa$, using eq 2 and 3; see below.

Calculations with molecular models can be used to illustrate the relatioships among the functions defined above. For example, for dilute suspensions of dumbbell particles, Bird and co-workers[7] give relations for small $\tau_c\kappa$ (for $\eta_0$ much greater than the solvent viscosity) that can be put in the forms of eq 2–4 with

$$Q(\tau_c\kappa) = 1 - 1.428(\tau_c\kappa)^2 + 5.3151(\tau_c\kappa)^4 - \ldots \tag{13}$$

$$P(\tau_c\kappa) = 1 - 1.179(\tau_c\kappa)^2 + \ldots \tag{14}$$

$$N(\tau_c\kappa) = 1 - 0.159(\tau_c\kappa)^2 + \ldots \tag{15}$$

Consequently, with this model $P$ and $N$ are not expected to be equal (unless $\tau_c\kappa = 0$). Approximate closed expressions for $Q$ and $N$ calculated for rodlike chains by Doi and Edwards[8] will be discussed below. For this calculation, the coefficients −1.43 and −0.16 in eq 13 and 15 are replaced by −1.34 and +0.93, respectively.

## Experimental Section

As in cone-and-plate rheometer used to determine the steady-state viscosity and recoverable compliance as functions of shear rate has been described in detail elsewhere.[9] The instrument employs an inert cone and plate, a wire-suspended cone mounted coaxially with a drag-cup torque transducer, and a plate that may be rotated at precisely controlled angular velocity $\Omega$. The drag-cup transducer generates the restoring torque $M$ required to hold the cone stationary in steady-state flow. In recovery measurements, both $M$ and $\Omega$ are set equal to zero, and the rotational angle $\varphi_R$ of the cone in recovery is determined. The

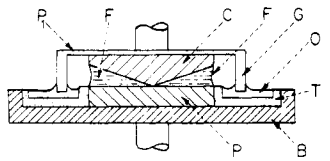


**Figure 1.** Schematic drawing of the cone–plate assembly: P, plate attached to a spindle that can be rotated at angular velocity Ω; C, cone attached to drag-cup tranducer and suspended by wire supports; F, fluid; B, base plate; T, trough for sealant oil; O, sealant oil; G, glass cylinder dipping into sealant oil; $P_1$, support for G.

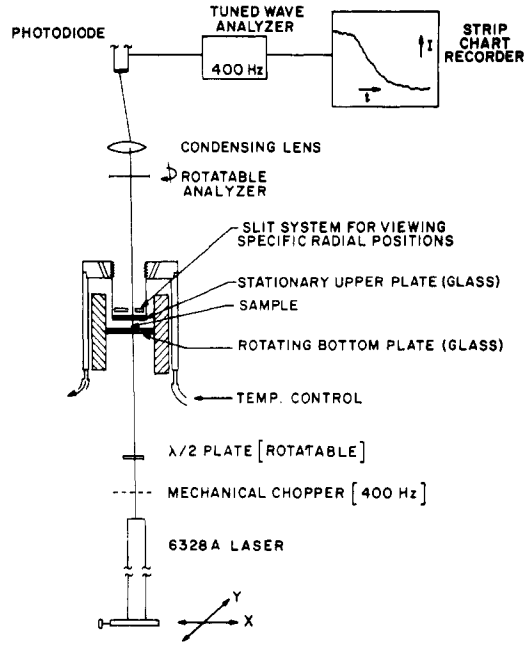


**Figure 2.** Schematic drawing of flow birefringence apparatus showing its principal parts as indicated.

viscosity and the shear rate are calculated with the ususal relations for cone-and-plate deformation with torque $M$ and angular velocity Ω of the plate relative to the cone[10a]

$$\eta_\kappa = \sigma/\kappa \tag{16}$$

$$\sigma = 3M/2\pi r^3 \tag{17}$$

$$\kappa = \Omega/\Theta \tag{18}$$

Here Θ is the angle between the cone and plate and $r$ is the radius of the cone. The recoverable compliance is calculated from the ultimate recoverable strain $\gamma_R$ determined by the ultimate angular recovery $\varphi_R$ following cessation of steady-state flow under shear stress

$$R_\kappa = \gamma_R/\sigma \tag{19}$$

$$\gamma_R = \varphi_R/\Theta \tag{20}$$

As in previous experiments,[3] a positive pressure of dry nitrogen is maintained in the rheometer to inhibit contamination of the solution by moisture, but, in addition, the cone–plate assembly is surrounded by a glass ring dipped into an oil-filled trough to seal the test solution; see Figure 1. Mineral oil, dried by contact with sulfuric acid is used in the trough. The presence of the oil did not add significantly to the measured torque $M$ and had no effect on $\varphi_R$.

Flow birefringence measurements were made with a parallel-plate apparatus, shown schematically in Figure 2. The lower plate is rotated with angular velocity Ω, while the upper plate is stationary. In this arrangement, the shear rate varies linearly with the distance from the center of rotation and inversely with the separation $h$ of the plates[10b]

$$\kappa = (r/h)\Omega \tag{21}$$

A light beam was directed perpendicular to the plane of the plate (the so-called 1–3 plane, where 1 is the flow direction and 2 is the direction of gradient)[5] for measurement. Optical measurements were performed with an analyzer placed with its transmission axis at angle $\beta$ to that of a polarizer placed in the incident beam. Since the birefringence under study is relatively large, it was sufficient to use schlieren-grade glass windows for the plates and polaroid polarizers. The birefringence $\Delta n_{13}$ was determined by one of two methods. In one method, a polarized beam from a He–Ne laser is transmitted through an area of diameter $d$ = 1.5 mm with its center located at radial position $r$ and azimuthal angle $\alpha$ measured from the transmission axis of the analyzer. With $\gamma$ the angle between the axis of the polarizer and the unique axis ($n_1$) of the refractive index ellipsoid, the transmission $T$ is given by[11,12]

$$T = \tfrac{1}{2}\sin^2(\delta/2)(1 - \cos 4\gamma) \tag{22}$$

for $\beta = \pi/2$, where $\delta$ is the retardation

$$\delta = 2\pi h\Delta n_{13}/\lambda \tag{23}$$

($\delta$ in radians) with $\lambda$ the wavelength of the incident light in a vacuum.

According to eq 22, $T$ is zero when $\gamma$ is $m\pi/2$, $m$ = 0, 1, 2, or 3. For birefringence in the 1–3 plane, one expects[13] an extinction isocline ($T$ = 0) for azimuthal angles $\alpha = m\pi/2$, $m$ = 0, 1, 2, or 3, as is observed with the solutions under study, so that $\cos 4\gamma = \cos 4\alpha$. When $\delta$ is equal to $2\pi$, $T$ is zero for all $\alpha$, so that an extinction circle is observed. To determine $\delta$ for $\delta$ not equal to $2\pi$, $\gamma$ is set to $\pi/4$, and the transmission is monitored by the responses $G_\epsilon$ and $G_0$ of a photodiode placed above the analyzer, with $\beta = \pi/2$ for the sample in flow and $\beta = \pi/2 - \epsilon$ for the quiescent fluid, respectively, to give

$$\sin^2(\delta/2) = (G_\epsilon/G_0)\sin^2\epsilon \tag{24}$$

from which $\delta$ may be determined. In another method sometimes used to determined $\delta$, a quarter-wave plate is placed between the fluid and the analyzer, oriented with its slow direction parallel to the transmission axis of the polarizer. Under these conditions, the transmission is given by

$$T = \cos^2\beta + \tfrac{1}{2}\sin 2\beta \sin 2\gamma - \tfrac{1}{2}\cos 2\beta \sin^2(\delta/2)(1 - \cos 4\gamma) \tag{25}$$

With $\delta - 2\beta = \pi$, eq 25 exhibits twofold symmetry

$$T_{\delta-2\beta=\pi} = \tfrac{1}{2} + \tfrac{1}{2}\cos\delta(1 - \sin^2 2\gamma) - \tfrac{1}{2}[\sin^2\delta \sin 2\delta + \cos^2\delta \sin^2 2\gamma] \tag{26}$$

Consequently, adjustment of $\beta$ to an angle that results in a twofold symmetric pattern with extinction for $\gamma = \pi/4$ and $3\pi/4$ provides a means to determine $\delta$.

With the photometric method to determine $\delta$, the coordinates $r$ and $\alpha$ are set by translation of the incident beam by a mirror mounted on an $x$–$y$ stage. A circular diaphragm centered at the $r$, $\alpha$ position above the fluid serves to reduce stray light contribution to $G$. The laser is mounted so that the plane of polarization forms a dihedral angle of 45° with the plane of the positioning mirror. The polarization of the incident beam is adjusted by a half-wave plate placed between the mirror and the sample. The light beam is modulated at 400 Hz by a mechanical chopper, and the output from the transducer is monitored with a Hewlett-Packard Model 501 wave analyzer tuned to the modulation frequency. This procedure eliminates contributions from room light. The angles $\beta$ and $\epsilon$ are adjusted to within 0.5°, which is satisfactory for our purpose.

When the quarter-wave plate is used to determine $\delta$, the sample is illuminated with a collimated beam from a zirconium arc lamp. The angle $\beta$ is reproducible to within 0.2° for this measurement. Comparisons of $\delta$ determined by the two methods used here agreed within 0.05 rad.

The value of $\delta$ is used to calculate the birefringence $\Delta n_{13}$ with eq 23. According to Philippoff,[13] the observed birefringence $\Delta n_{13}$ is related to the difference $\Delta n$ of the principal components of the refractive index ellipsoid through the equation

$$\Delta n = (\Delta n_{13} - \Delta n_{23})/\cos 2\chi = \Delta n_{12} \tag{27}$$

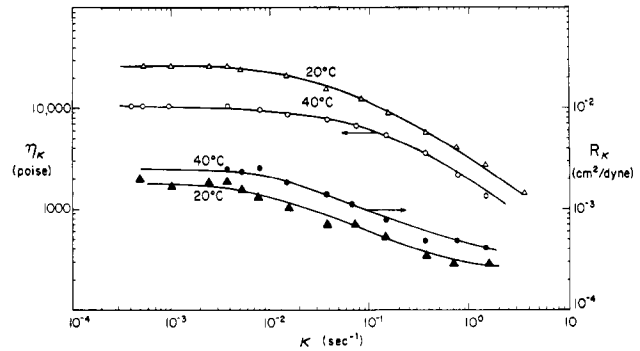


**Figure 3.** Representative plots for the viscosity $\eta_\kappa$ and recoverable compliance $R_\kappa$ as functions of shear rate $\kappa$. Data are for PBT-53 in methanesulfonic acid; $c$ = 0.0379 g/mL.

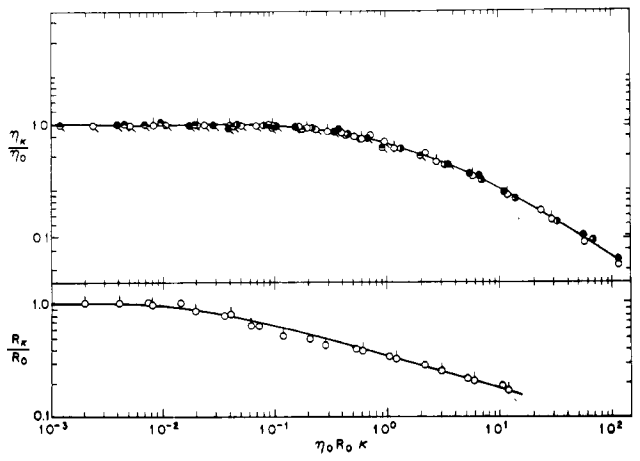


**Figure 4.** Reduced plots of $\eta_\kappa/\eta_0$ and $R_\kappa/R_0$ as functions of $\tau_c\kappa$ for solutions of PBT-62. Symbols ◑, ○, ⊖, and ● are for data at 80, 60, 40, and 20 °C, respectively, with pips indicating concentration as ○, ◇, and ○ for 0.015, 0.0252, and 0.030 weight fraction, respectively. The solid curve in $\eta_\kappa/\eta_0$ vs. $\tau_c\kappa$ represents data for polyisobutylene in cetane, shown for comparison.

where the birefringence $\Delta n_{23}$ in the 2–3 plane is usually very small, and $\Delta n_{12}$ is the birefringence in the 1–2 plane. The strong absorption of light by the solutions under study prohibits direct measurement of $\Delta n_{12}$, for example, by Couette flow, which is the more usual method to study birefringence.[5] Relatively few examples of birefringence measurements in the 1–3 plane exist.[14]

**Materials.** All polymers were used without fractionation, owing to the tendency for increased interchain association with fractionated samples. The polymers were obtained from several sources: the PBO polymers from Dr. F. E. Arnold, Materials Branch, Air Force Materials Laboratory; the PBT polymers from Dr. J. F. Wolfe, SRI International; and the PPTA from Dr. C. Strazielle, Centre de Recherches sur les Macromolecules, Strasbourg, France (see ref 15); a sample of Kevlar 49 was made available by Dr. J. R. Schaefgen, E. I. du Pont de Nemours and Company.

The polymers have been characterized by light scattering and viscosity measurements[15,16] on dilute solutions, with the results given in Table I.

Solutions were prepared by addition of the appropriate quantities of dry polymer and distilled solvent to a 35-mL tube containing a Teflon-coated magnetic stirring bar. The tube was sealed and suspended between the poles of a magnet. The tube was immersed in oil held in a copper vessel that also fitted between the poles of the magnet. Slow stirring action was achieved by rotating the sample tube with the stirring bar held fixed by the magnet. The oil bath was raised to 60 °C to facilitate mixing.

## Results

Although it is possible to form nematic solutions with each of the polymers used in this study, the present investigation is confined to solutions which are optically isotropic at rest. Some typical data for $\eta_\kappa$ and $R_\kappa$ vs. $\kappa$ are shown in Figure 3. The data are reduced to plots of $\eta_\kappa/\eta_0$ and $R_\kappa/R_0$ vs. $\eta_0 R_0 \kappa$ to give the results shown in Figures 4–6, using the parameters $\eta_0$ and $R_0$ given in Table II. For

Table I
Characterization of Polymers Used in This Study

| polymer | no. | $[\eta]$,[a] dL/g | $M_w$ | $L_w$,[b] nm |
|---|---|---|---|---|
| PBT | 62 | 26.5 | 37 000 | 168 |
| | 53 | 14.0 | 26 000 | 118 |
| | 43 | 9.5 | 21 000 | 96 |
| | 20 | 6.0 | 16 200 | 74 |
| | 38-B | 5.1 | 15 000 | 68 |
| PBO | 2 | 2.68 | 12 500 | 68 |
| PPTA | 6 | 7.4 | 47 000 | 250 |
| | 2 | 2.7 | 16 000 | 85 |

[a] The low shear rate limiting value determined in methanesulfonic acid at 25 °C. [b] $L_w$ calculated as $M_w/M_L$. $M_L$ is 220 nm$^{-1}$ for PBT, 183 nm$^{-1}$ for PBO, and 189 nm$^{-1}$ for PPTA.

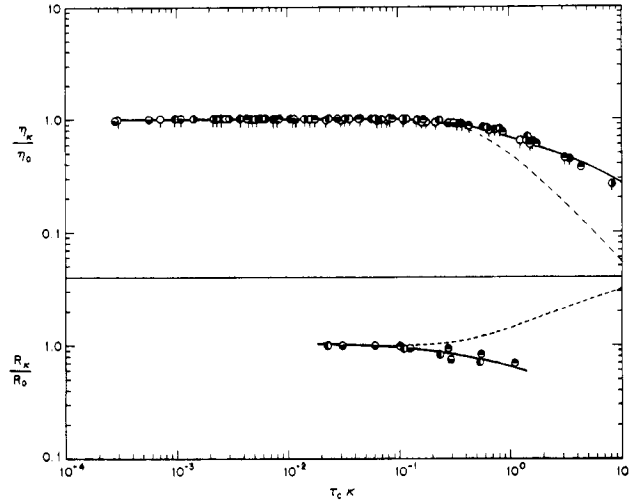


**Figure 5.** Reduced plots of $\eta_\kappa/\eta_0$ and $R_\kappa/R_0$ as functions of $\tau_c\kappa$ for solutions of PPTA-6. Symbols ○, ●, ⊖, ◐, ⊖, and ⊖ are for data at 60, 40, 24, 20, 10, and 0 °C, respectively, with pips indicating concentrations as ○ and ○ for 0.053 and 0.060 weight fractions, respectively. Solid curve in $\eta_\kappa/\eta_0$ vs. $\tau_c\kappa$ as in Figure 4. Dashed curves represent the theory of Doi and Edwards for $\eta_\kappa/\eta_0$ and $S_\kappa/S_0$ vs. $\tau_c\kappa$.

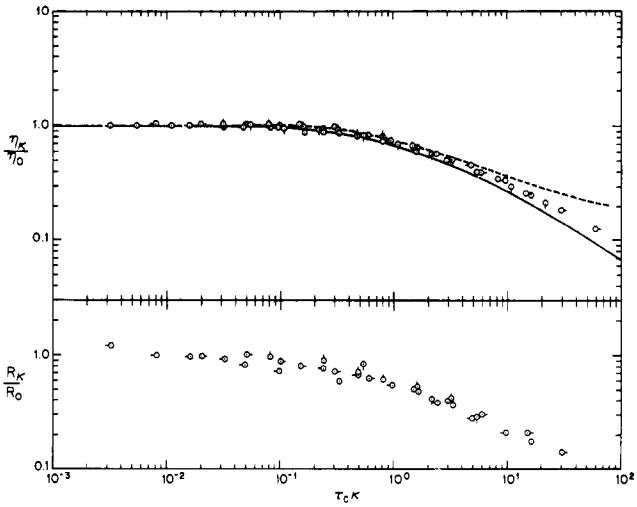


**Figure 6.** Reduced plots of $\eta_\kappa/\eta_0$ and $R_\kappa/R_0$ as functions of $\tau_c\kappa$ for solutions of PBT-53 with 0.0255 weight fractions at (⊙) 60, (○) 40, (⊙) 30, (⊙) 23, and (⊙) 12.5 °C. Solid curve in $\eta_\kappa/\eta_0$ vs. $\tau_c\kappa$ as in Figure 4. Dashed curve represents calculation of Cohen.

Table II
Rheological Parameters for
Rodlike Polymer Solutions ($T$ = 20 °C)

| polymer | no. | solvent[a] | $c$, g/mL | $\eta_0$, P | $R_0$,[b] cm²/dyn |
|---|---|---|---|---|---|
| PBT | 62 | MSA + CSA | 0.0222 | $0.42 \times 10^4$ | $(11) \times 10^{-4}$ |
| | 62 | MSA + CSA | 0.0373 | 45 | 10 |
| | 62 | MSA + CSA | 0.0444 | 79 | 12 |
| | 53 | MSA + CSA | 0.0428 | 0.56 | 8 |
| | 43 | MSA + CSA | 0.0489 | 0.082 | 4.5 |
| | 53 | MSA | 0.0377 | 2.2 | 18 |
| | 53 | MSA | 0.0379 | 2.8 | 22 |
| | 53 | MSA | 0.0408 | 12 | 16 |
| | 53 | MSA | 0.0435 | 8.0 | 19 |
| | 53 | MSA | 0.0444 | 14 | 14 |
| | 43 | MSA | 0.0454 | 0.26 | 18 |
| | 38-B | MSA | 0.0446 | 0.027 | 25 |
| | 20 | MSA | 0.0476 | 5.7[c] | 18 |
| PBO | 2 | MSA | 0.061 | 0.0085 | |
| | | MSA | 0.075 | 0.026 | |
| | | MSA | 0.090 | 0.055 | |
| | | MSA | 0.105 | 0.13 | |
| PPTA | 6 | MSA | 0.0340 | 0.103 | 1.2 |
| | | MSA | 0.0474 | 0.209 | 0.7 |
| | | MSA | 0.0518 | 0.279 | 0.7 |
| | | MSA | 0.0740 | 0.873 | 0.5 |
| | | MSA | 0.0784 | 0.923 | 0.4 |
| | | MSA | 0.1006 | 4.58 | 0.5 |
| | | MSA | 0.123 | 12.5 | 0.5 |
| | | MSA | 0.151 | 61.2 | (0.5) |
| | 2 | MSA | 0.0944 | 0.0070 | |

[a] MSA and CSA are methanesulfonic acid and chlorosulfonic acid, respectively. MSA + CSA is a mixture with 3% CSA in 97% MSA. [b] Values in parentheses are obtained as $\tau_c \eta_0^{-1}$, where $\tau_c$ is estimated from the dependence of $\eta_\kappa$ on $\kappa$, as described in the text. [c] Values determined for a 1-year-old solution (see text).

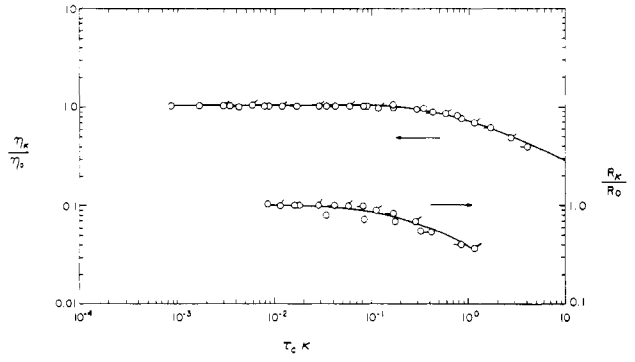


**Figure 7.** Reduced plots of $\eta_\kappa/\eta_0$ and $R_\kappa/R_0$ as functions of $\tau_c\kappa$ for a solution of Kevlar 49 in methanesulfonic acid with a 0.0628 weight fraction at (○) 40, (◑) 20, and (◐) 10.5 °C. Values of $\eta_0$ are 3800, 10 800, and 17 000, respectively, at these temperatures, and values of $\tau_c$ are 0.220, 0.702, and 1.105, respectively. The solid curve in $\eta_\kappa/\eta_0$ vs. $\tau_c\kappa$ as in Figure 4.

comparison purposes, reduced data observed with solutions of Kevlar 49 are shown in Figure 7. It may be seen that the data for both $\eta_\kappa/\eta_0$ and $R_\kappa/R_0$ at different temperatures and concentrations superpose quite well. The reduced curves for the different polymers are similar. Additional data on other compositions corresponding to the entries in Table II are quantitatively similar and are not shown. The solid curve shown for $\eta_\kappa/\eta_0$ vs. $\eta_0 R_0 \kappa$ in Figures 4–7 corresponds to the reduced curve for a solution of the flexible-chain polymer polyisobutylene in cetane,[3] illustrating the insensitivity of the reduced flow curve to details of the molecular structure.

With two samples, $R_0$ could not be determined with the rheometer in use. In such cases, values of $R_0$ entered in Table II were estimated by comparison of $\eta_\kappa/\eta_0$ vs. $\eta_0\kappa$ with

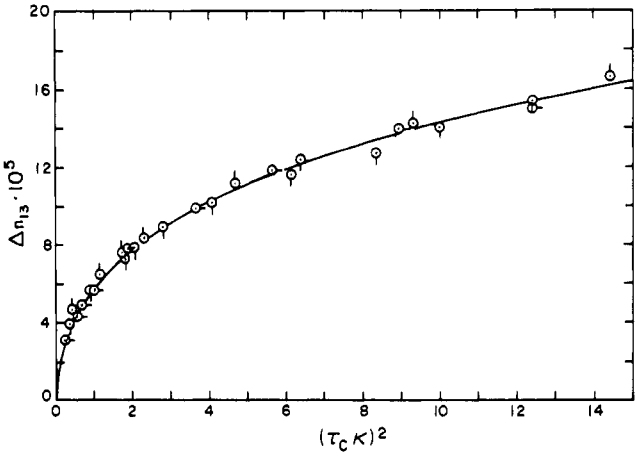


**Figure 8.** Birefringence $\Delta n_{13}$ as a function of the reduced shear rate $\tau_c\kappa$ for a PBT solution with 0.0255 weight fraction: (○) 40; (◑) 23; (◐) 10 °C.

the reduced curve for the same polymer at some other concentration and/or temperature as noted in Table II.

Data for $\Delta n_{13}$ vs. $(\tau_c\kappa)^2$ are shown in Figure 8 for a PBT solution. According to eq 27, $\Delta n_{13}$ is equal to $\Delta n \cos 2\chi + \Delta n_{23}$, with the latter expected to be small. For small $\tau_c\kappa$ (or more precisely, for what Coleman and co-workers have termed "slow flows"[2,6]), both $\Delta n$ and $\cos 2\chi$ should be proportional to $\tau_c\kappa$

$$\Delta n = 2CR_0^{-1}\tau_c\kappa + \ldots \quad (28)$$

$$\cot 2\chi = \tau_c\kappa + \ldots \quad (29)$$

$$\Delta n_{13} \simeq \Delta n \cos 2\chi = 2CR_0^{-1}(\tau_c\kappa)^2 + \ldots \quad (30)$$

where the equality of $R_0$ and $S_0$ has been used. Although Coleman and co-workers have noted that there is no fundamental reason for $C$ to be independent of $\kappa$ except when $\kappa$ is very small and suggest that such behavior does not obtain with precision for "second-order fluids", here it is only necessary to note that plots of $\Delta n_{13}$ vs. $\tau_c\kappa$ appear to superpose reasonably well over the range of temperature studied, as may be seen in Figure 8. It is evident from the data in Figure 8 that the limiting behavior expected for small $\tau_c\kappa$ is not reached for the $\tau_c\kappa$ range employed; see below.

## Discussion

**Linear Viscoelastic Properties.** The limiting viscosity $\eta_0$ of the moderately concentrated isotropic solutions of PBT, PBO, and PPTA increases markedly with increasing polymer concentration, even though the solutions are far removed from any glass transition. The latter is evident, for example, since the ratio $\eta_0/\eta_s$ of solution to solvent viscosities is independent of temperature. The strong dependence of $\eta_0$ on concentration can be understood in terms of a model described by Doi and Edwards[8] which attributes the marked dependence of $\eta_0$ on $c$ and $L$ to the effects of intermolecular interaction that act to suppress the rotatory diffusion of the rodlike chains. The phase transition to the ordered state is attributed to the same kind of interaction for volume fractions $\varphi > \varphi_c$ in the thermodynamic model of Flory.[1] Doi and Edwards limit their viscoelastic treatment to the concentration range $\varphi < \varphi_c$. In particular, they limit their treatments to concentrations in the range

$$1/[\eta] \ln (L/d) < c < 2/3A_2M < c_c \quad (31)$$

where $c$ is the concentration in weight per unit volume ($c = \rho\varphi$, with $\rho$ the solute density) and $A_2$ is the second virial

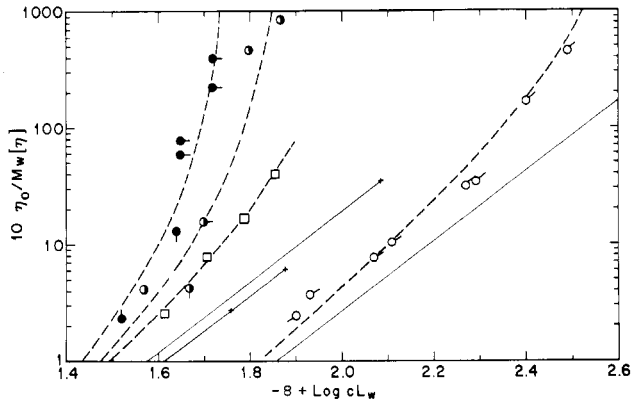


**Figure 9.** Ratio $\eta_0/M_w[\eta]$ of the zero shear rate viscosity $\eta_0$ to $M_w[\eta]$ as a function of the product $cL_w$ of polymer concentration and contour length (all in cgs units) for (○) PBT-62, (◔) PBT-53, (◔) PBT-43, (◔) PBT-20, (◔) PBT-38-B, (□) PBO-2, (◔) PPTA-6, and (◔) PPTA-2. Half-filled circles are for solutions in methanesulfonic acid containing 3% chlorosulfonic acid; otherwise data are for solutions in methanesulfonic acid. The dashed curves represent eq 35 and 36 as described in text. The solid lines represent the limit for this behavior with $f(\nu/\nu^*)$ in eq 36 equal to unity; each line terminates at $c^*L_w/B$, corresponding to the value of $cL_w$ for which $\eta_0/M_w[\eta]$ is a maximum.

coefficient. According to Doi and Edwards, in the specified range, $\eta_0$ is given by the expression

$$\eta_0 = \nu kT/10D_R \tag{32}$$

where the number $\nu$ of rods per unit volume is given by $\nu = cN_A/M$ and the rotational diffusion constant $D_R$ at concentration $\nu$ is given (in the range defined by eq 31) by

$$D_R^{-1} = (\nu L^3)^2 f(\nu/\nu^*)/\beta D_R^0 \tag{33}$$

with $\beta$ a constant about equal to unity, $f(\nu/\nu^*)$ a function that is unity for $\nu \ll \nu^*$ and increases with increasing $\nu$, where $\nu^*$ is about equal to $\rho\varphi_c N_A/M$ (see below), and $D_R^0$ the diffusion constant at infinite dilution, proportional to $L^3$

$$kT/D_R^0 \propto M[\eta]\eta_s \tag{34}$$

where $[\eta]$ is the intrinsic viscosity and $\eta_s$ is the viscosity of the solvent. Equations 32–34 are conveniently combined in the form

$$\eta_0/\eta_s = KM[\eta](cL/M_L)^3 f(cL/M_L\gamma^*) \tag{35}$$

with $\gamma^* = c^*L/M_L$, where $L$ and $d$ are the (contour) length and diameter of the (monodispersed) rodlike chain with mass per unit length $M_L = M/L$ and $K$ is a constant. The factor $M_L$ appears in eq 35 since $D_R/D_R^0$ involves $\nu L = cN_A/M_L$, whereas eq 35 is expressed in terms of the mass per unit volume concentration $c$. According to eq 35, $\eta_0/M[\eta]$ is expected to depend only on $cL$ for a homologous series, to the extent that $\gamma^*$ is a constant. If $c^*$ is identified with $\rho\varphi_c$, then $\gamma^*$ is $\rho Ad/M_L$ and should be constant.

Data for the viscosity are plotted vs. $cL_w$ in Figure 9. (The weight-average chain length is used for convenience.) The results show that the expected region of proportionality of $\eta_0/M_w[\eta]$ with $(cL_w)^3$ for $c \ll c^*$ is only found with the lowest concentrations of the PBT solutions used. According to Doi,[17] a reasonable approximation to $f(\nu/\nu^*)$ is given by the relation

$$f(\nu/\nu^*) = (1 - B\nu/\nu^*)^{-2} \tag{36}$$

where $B$ is a little smaller than unity. With the use of eq 36, $\eta_0/M[\eta]$ exhibits a slow crossover from proportionality with $(cL)^3$ for $c/c^*$ less than about 0.5 to proportionality with $(cL)^m$ for larger $c/c^*$, where $m$ is greater than 3 and

Table III
Viscometric and Thermodynamic Parameters for Solutions of Rodlike Polymers

| polymer | no. | solvent[a] | $c^*/B$, g/mL | $\rho\varphi_c$, g/mL |
|---|---|---|---|---|
| PBT | 53 | MSA | 0.0488 | 0.0452 |
| | 43 | MSA | 0.0600 | |
| | 38-B | MSA | 0.0846 | |
| PBT | 62 | MSA + CSA[b] | 0.0452 | 0.047 |
| | 53 | MSA + CSA | 0.0643 | |
| | 43 | MSA + CSA | 0.0790 | |
| PBO | 2 | MSA | 0.180 | 0.178 |
| PPTA | 6 | MSA | 0.196 | |
| | 2 | MSA | 0.578 | |

[a] MSA = methanesulfonic acid; CSA = chlorosulfonic acid. [b] 3% CSA by weight.

depends on $B$. The experimental data exhibit a fairly sharp crossover, with $m$ approaching a value of 10 or more, which would require $B$ to be nearly unity.

Inspection of Figure 9 shows that the various sets of data do not reduce to a single function of $\eta_0/\eta_s M[\eta]$ vs. $cL_w/M_L$, as should be expected from eq 35 if $\gamma^*$ is identical for all solutions and $M_L$ is equal to $m_0/l$, where $m_0$ and $l$ are the mass and length, respectively, of a repeating unit. It may be mentioned that data of Baird et al.[18] on solutions of PPTA in 100% sulfuric acid are similar to the results reported here for PPTA in methanesulfonic acid. Both sets of data give much smaller $\eta_0/\eta_s M_w[\eta]$ at a given $cL_w/M_L$ than is observed for PBT or PBO.

The dependence of $\eta_0/\eta_s M_w[\eta]$ on $cL_w$ is closely correlated with the concentration $c_c = \rho\varphi_c$ for the onset of the ordered anisotropic phase. Thus, the dashed lines in Figure 9 represent eq 35 with eq 36 for $f(\nu/\nu^*)$, using the parameters $c^*/B$ given in Table III. For each dashed curve, $c^*L_w/B$ is a constant. The comparisons of $c^*/B$ with $c_c$ given in Table III indicate that $Bc_c/c^*$ is nearly unity or that $B$ is close to unity, as suggested by Doi, if $c^* = c_c$. Evidently, factors responsible for the disparity of the dependence of $\eta_0/\eta_s M_w[\eta]$ on $cL_w$ among the systems studied are also acting to affect $c_c$. For example, $c_c$ seems a little smaller for a solution in pure methanesulfonic acid as compared with a solution in the same solvent containing 3% chlorosulfonic acid.

Several factors could be responsible for the disparate behavior just described, including (1) molecular weight polydispersity, (2) partial flexibility of the chain, (3) intermolecular interactions (electrostatic etc.), and (4) intermolecular association. Although the samples are not fractionated, available information[15] indicates comparable molecular weight distribution, so that large effects causing differences on $c_c$ would be unexpected. Moreover, in some cases, $c_c$ is different for a given polymer in different solvents. Light scattering characterization in dilute solution indicates that[15,19] PBT and PBO have the rodlike nature expected and that PPTA has a persistence length $\rho$ of about 80 nm, so that $L/\rho$ is about 4 for the PPTA polymers studied. It is possible that this degree of flexibility accounts for part, or all, of the decreased viscosity of PPTA in comparison with PBT.

The possible effects of intermolecular association cannot be dismissed and might affect both $\eta_0$ and $c_c$ in the manner observed. For example, effects observed on $[\eta]$ have been interpreted in terms of association with the chains having their axes in parallel array.[19] For a small extent of such association, the effects are to increase $M_L$ and decrease $\nu$ by the same extent and to increase $d$, probably by a factor somewhat smaller than the change in $M_L$. For polydispersed rodlike chains, the effect on the average length

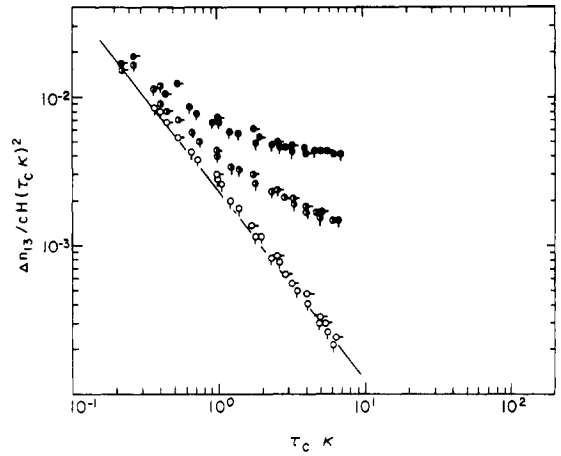


**Figure 10.** Flow birefringence plotted as $\Delta n_{13}/cH(\tau_c\kappa)^2$ for $c$ = 0.0408 g/mL as a function of reduced shear rate $\tau_c\kappa$. Here $H$ is unity for unfilled circles, $Q^2$ for the half-filled circles, and $PQ^2$ for the filled circles: (Q) 60; (O) 40 °C.

might not be very large. If these conditions obtain, then the effects of association will appear as a horizontal shift of the data in Figure 9 by an amount equal to the difference in logarithms of $M_L$ for the dissociated and associated chains. This analysis indicates that the degree of association is about 1.3 and 1.7 for PBT in methanesulfonic acid containing 3% chlorosulfonic acid and for PBO in methanesulfonic acid, respectively, using the behavior of PBT in methanesulfonic acid as a base of comparison. If the larger displacement for PPTA solutions is explained in terms of association rather than deviation from a rodlike conformation, then the degree of association increases from 2 to 7 with increasing polymer concentration. At the present time, we cannot distinguish definitely between these alternative interpretations.

Finally, we remark that in one case the viscosity of a solution of PBT-20 in methanesulfonic acid (0.048 g/mL) measured after being stored for 1 year was found to be about 100-fold greater than expected. This behavior may reflect the type of random association that has been observed with other rodlike chains.[3b]

The model of Doi and Edwards used to compute $\eta_0$ also yields the Rouse-like result

$$S_0 = 5/3\nu kT = 5M/3cRT \tag{37}$$

With the assumption that $R_0 = S_0$, this relation gives

$$\tau_c = \eta_0 R_0 = (6D_R)^{-1} \tag{38}$$

for the time constant. Comparison of the experimental $R_0$ with eq 37 is hampered by the unknown, and usually large, effects of molecular weight dispersity on $R_0$. With PBT, the experimental $R_0$ are larger than calculated with eq 37, an effect that might be attributed to molecular weight heterogeneity. In addition, the dependence of $R_0$ on $c$ does not follow the inverse dependence on $c$ expected with eq 37. The weak dependence of $R_0$ on $c$ is in accord with previous observations[19] on PBO solutions for which $R_0$ exhibited a minimum with increasing $c$ for $c$ a little less than $c_c$. We are unaware of a theoretical treatment which exhibits this behavior.

As remarked above, the data on $\Delta n_{13}$ do not extend to low enough $\tau_c\kappa$ to obtain linear behavior, and the limiting value of $\Delta n_{13}/(\tau_c\kappa)^2$. This is evident in the bilogarithmic plot of $\Delta n_{13}/c(\tau_c\kappa)^2$ vs. $\tau_c\kappa$ given in Figure 10. Quantitatively, similar results were obtained for the data shown in the linear plot in Figure 8. It can be concluded that the limiting value of $\Delta n_{13}/c(\tau_c\kappa)^2$ for small $\tau_c\kappa$ is larger than 0.02 mL/g. It is of interest to compare this estimate with the result expected for a dilute solution of rodlike molecules, for which[20]

$$\lim_{\substack{\tau_c\kappa=0 \\ c=0}} \Delta n/c = (2/5)(\Delta n_\infty/c)\tau_c\kappa \tag{39}$$

where $\Delta n_\infty/c$ is given by

$$\Delta n_\infty/c = 3\delta(\partial n/\partial c) \tag{40}$$

with $\delta$ and $\partial n/\partial c$ the molecular anisotropy and refractive index increment, respectively, of the polymer in solution. The latter may be expressed in terms of the principal refractive indices $n_1$ and $n_2$ through the parameters

$$4\pi g_i = \frac{n_i^2 - n_s^2}{1 + (n_i^2 - n_s^2)L_i/4\pi n_s^2} \tag{41}$$

as

$$\delta = (g_1 - g_2)/(g_1 + 2g_2) \tag{42}$$

$$\partial n/\partial c = (2\pi/3n_s)(g_1 + 2g_2)\bar{v} \tag{43}$$

Here $n_s$ is the solvent refractive index, $\bar{v}$ is the partial specific volume of solute, and the form factor $L_i$ is given by $L_1 = 0$ and $L_2 = 2\pi$ for rods. Values of $\delta$ and $\partial n/\partial c$ are 0.6 and 0.55 mL/g, respectively, for PBT in methanesulfonic acid,[15] and, apparently, $n_1 \neq n_2 \neq n_s$. These data give $\Delta n_\infty/c$ equal to 1.0 mL/g for PBT in methanesulfonic acid.

These results give the estimate 0.4 mL/g for the limiting value of $\Delta n_{13}/c(\tau_c\kappa)^2$, in comparison with the value 0.02 mL/g observed for the smallest $\tau_c\kappa$ used. The large discrepancy may merely mean that the limiting behavior is not reached until $\tau_c\kappa$ is very small or may indicate that for the moderately concentrated solutions studied here, $\Delta n_\infty$ is not as large as the dilute-solution limit given by eq 40 or that other effects, such as the polydispersity of molecular weight of the samples used, act to reduce $\Delta n_{13}$. It may be noted that the power law behavior for $\Delta n_{13}/c(\tau_c\kappa)^2$ given in Figure 10 extrapolates to $\Delta n_{13}/c(\tau_c\kappa)^2$ equal to 0.4 for $\tau_c\kappa$ equal to 0.02. We will return to the nonlinear behavior of $\Delta n_{13}$ below.

**Nonlinear Viscoelastic Properties.** The data in Figures 4–7 exhibit the reduced plots for the nonlinear behavior observed for isotropic solutions of the polymers studied. The satisfactory reduction of the data in terms of the parameter $\tau_c\kappa$ is one noteworthy result. The theory of Doi and Edwards[8] gives results that can be expressed in the form

$$Q(\tau_c\kappa) = [1 + A_\eta(\tau_R\kappa)^2]^{-0.525} \tag{44}$$

$$N(\tau_c\kappa) = [1 + \alpha_\eta(\tau_R\kappa)^2]^{1.050}/[1 + A_s(\tau_R\kappa)^2]^{0.874} \tag{45}$$

with $\tau_R$ equal to $(6D_R)^{-1}$, $A_\eta = 2.556$, and $A_s = 2.009$ (for monodisperse solute). With eq 38, $\tau_R = \tau_c$, permitting the direct comparison of experiment and theory shown in Figure 5. The result shows that eq 44 decreases more rapidly with increasing $\tau_c\kappa$ than does the experimental data. A revised calculation with the Doi–Edwards model due to Cohen[21] provides a closer fit to the experimental results, as shown in Figure 6. The revised calculation, which retains terms dropped in the original version, decreases more slowly with increasing $\tau_c\kappa$, in accord with experiment.

We are unaware of any calculation of $P$ for moderately concentrated solutions of rodlike chains. The theoretical results of Doi and Edwards for monodispersed rodlike chains give $N$ that increases with increasing $\tau_c\kappa$, the increase becoming noticeable for $\tau_c\kappa$ greater than about unity. For coiled polymers, the functions $P$ and $N$ are similar, at

least for $\tau_c\kappa$ not much larger than 10. By contrast, $P$ given in Figures 4–7 is far different from the calculated $N$, with $P$ decreasing with increasing $\tau_c\kappa$ for $\tau_c\kappa$ greater than about 0.01. It is possible that much of this difference can be ascribed to the effects of molecular weight dispersity, which is known to cause similar behavior for coiled polymers.

In the nonlinear response range, as mentioned above, eq 11 and 12 are often rewritten with $\eta_0$ and $S_0$ replaced by $\eta_\kappa$ and $S_\kappa$, respectively, to approximate the effects of nonlinear behavior in the birefringence.[5] These substitutions give

$$\Delta n_{13} \simeq 2C'R_0^{-1}NQ^2(\tau_c\kappa)^2 \tag{46}$$

with

$$C' = C(\cot 2\chi)/S_\kappa\eta_\kappa\kappa \tag{47}$$

It appears that $C'$ is sometimes independent of $\kappa$, even for $\kappa$ greater than $\tau_c^{-1}$.[22] Since neither $\chi$ nor $N$ was determined in this study, we have examined a variation of these relations given by

$$\Delta n_{13} = 2C''R_0^{-1}PQ^2(\tau_c\kappa)^2 \tag{48}$$

where

$$C'' = C'N/P \tag{49}$$

is expected to equal $C$ as $P = N$ and $C' = C$. Although $N$ and $P$ need not be equivalent for large $\tau_c\kappa$, they should approach each other for small $\tau_c\kappa$, so that $C''$ and $C$ should be equal, at least for small $\tau_c\kappa$. The bilogarithmic plot of $\Delta n_{13}/cPQ^2(\tau_c\kappa)^2$ shown in Figure 10 reveals that $2C''(R_0c)^{-1}$ tends to a constant for $\tau_c\kappa$ greater than about unity. For smaller $\tau_c\kappa$, $2C''(R_0c)^{-1}$ increases with decreasing $\tau_c$ in the range studied—presumably $2C''(R_0c)^{-1}$ reaches a limiting value $2C(R_0c)^{-1}$ for still smaller $\tau_c\kappa$. Quantitatively similar results obtain for the data shown in the linear plot in Figure 8. In the preceding, it was estimated that $\Delta n_{13}/c(\tau_c\kappa)^2$ would reach the limiting value expected by analogy with dilute-solution behavior for $\tau_c\kappa$ about 0.02. This is also the range required for $P$ to reach its limiting value of unity ($Q$ is essentially unity for $\tau_c\kappa$ smaller than unity).

Since normal stress data are not available, we do not know whether deviation of $C''$ from $C$ is related to failure of eq 46 or 47 or to deviation of $N$ from $P$. Most experiments designed to evaluate $C''$ have been confined to the range $\tau_c\kappa > 1$, owing to the difficulty of measuring small normal forces. In that range, $C''$ measured here is nearly constant but smaller than its value for $\tau_c\kappa < 1$. It is presumed that $C'$ ought to be independent of $\tau_c\kappa$, as is reported for flexible-chain polymers. If so, then the dependence of $C''$ on $\tau_c\kappa$ indicates (1) that in the range $\tau_c\kappa$ greater than about unity, $\partial \ln P/\partial \ln (\tau_c\kappa)$ and $\partial \ln N/\partial \ln (\tau_c\kappa)$ are equal so that $C''$ is independent of $\tau_c\kappa$ but (2) that the function $N$ reaches its limiting value (unity) at smaller $\tau_c\kappa$ than does $P$ for the rodlike polymers studied. It is possible that both of these effects might be attributed to molecular weight polydispersity.

## Conclusions

The rheological and rheooptical properties described above for the three rodlike polymers show both striking differences and similarities in comparison with behavior of flexible coil polymers. In the concentration range studied, $\eta_0/M[\eta]$ depends markedly on $cL_w$, with the quantity $\partial \ln (\eta_0/M[\eta])/\partial \ln cL_w$ increasing rapidly as $c$ approaches the concentration $c_c$ required for stability of an ordered phase of the rodlike polymer. As $c$ nears $c_c$, the overall dependence of $\eta_0$ on chain length becomes especially severe. These effects can be understood qualitatively with a model introduced by Doi and Edwards.

The time constant $\tau_c = \eta_0R_0$ also depends markedly on $cL_w$ through its proportionality with $\eta_0$. Nonetheless, when expressed in terms of the reduced shear rate $\tau_c\kappa$, the functions $\eta_\kappa/\eta_0$ and $R_\kappa/R_0$ are similar to the corresponding behavior observed with flexible-chain polymers over the range studied ($10^{-3} < \tau_c\kappa < 10^2$). The rheooptical behavior exhibits the expected increase in the birefringence with increasing $\tau_c\kappa$, reflecting orientation of the rodlike molecules in the flow field. The birefringence is nonlinear even for $\tau_c\kappa$ as low as 0.1, a range for which $\eta_\kappa/\eta_0$ is essentially unity, whereas $R_\kappa/R_0$ may still exhibit nonlinear behavior. Quantitative estimations of the extent of orientation from the birefringence is hampered by dependence of the modified stress-optical coefficient $C''$ on $\tau_c\kappa$ for small $\tau_c\kappa$. Nonetheless, it is clear that orientation is appreciable and still increasing for $\tau_c\kappa$ in the range 10.

**Acknowledgment.** It is a pleasure to acknowledge partial support for this study from the Division of Materials Research, National Science Foundation (Grant DMR79-19853), and the Materials Laboratory, Wright-Patterson Air Force Base (Contract F33615-79-C5034).

## References and Notes

(1) (a) Flory, P. J. *Proc. R. Soc. London, Ser. A* **1956**, *234*, 73. (b) Flory, P. J.; Frost, R. S. *Macromolecules* **1978**, *11*, 1126.
(2) Coleman, B. D.; Markovitz, H. *J. Appl. Phys.* **1968**, *35*, 1.
(3) (a) Berry, G. C.; Hager, B. L.; Wong, C.-P. *Macromolecules* **1977**, *10*, 361. Wong, C.-P.; Berry, G. C. *Polymer* **1979**, *20*, 229.
(4) Graessley, W. W. *Adv. Polym. Sci.* **1974**, *16*, 1.
(5) See, for example: Janeschitz-Kriegl, H. *Adv. Polym. Sci.* **1969**, *6*, 170.
(6) Coleman, B. D.; Dill, E. H.; Toupin, R. A. *Arch. Ration. Mech. Anal.* **1970**, *39*, 358.
(7) Bird, R. B.; Warner, H. R., Jr.; Evans, D. C. *Adv. Polym. Sci.* **1971**, *8*, 1.
(8) (a) Doi, M.; Edwards, S. F. *J. Chem. Soc., Faraday Trans. 2* **1978**, *74*, 560. (b) *Ibid.* **1978**, *74*, 918.
(9) Berry, G. C.; Wong, C.-P. *J. Polym. Sci., Polym. Phys. Ed.* **1975**, *13*, 1761.
(10) Coleman, B. D.; Markovitz, H.; Noll, W. "Viscometric Flows of Non-Newtonian Fluids"; Springer-Verlag: New York, 1966: (a) p 52; (b) p 54.
(11) Benoit, H. Thesis, University of Strasbourg, 1950.
(12) Zimm, B. H. *Rev. Sci. Instrum.* **1958**, *29*, 360.
(13) Philippoff, W. *Trans. Soc. Rheol.* **1961**, *5*, 163.
(14) (a) Dexter, F. D.; Miller, J. C.; Philippoff, W. *Trans. Soc. Rheol.* **1961**, *5*, 193. (b) Foreman, W. T. *J. Chem. Phys.* **1960**, *32*, 277. (c) Wahl, J.; Fischer, F. *Mol. Cryst. Liq. Cryst.* **1973**, *22*, 359. (d) *Opt. Commun.* **1972**, *5*, 344. (e) Skarp, K.; Carlson, T. *Mol. Cryst. Liq. Cryst.* **1978**, *49*, 75.
(15) Metzger, P. Ph.D. Thesis, Carnegie-Mellon University, Pittsburgh, PA, 1979.
(16) Metzger, P.; Cotts, D.; Berry, G. C., to be published.
(17) Doi, M. *J. Phys. (Paris)* **1975**, *36*, 607.
(18) Baird, D. G.; Ballman, R. L. *J. Rheol.* **1979**, *23*, 505.
(19) Wong, C.-P.; Ohnuma, H.; Berry, G. C. *J. Polym. Sci., Polym. Symp.* **1978**, *65*, 173.
(20) See, for example: Tsvetkov, V. N., et al. "Structure of Macromolecules in Solution" (English Translation); National Lending Library for Science and Technology: Boston Spa, England, 1971; Vol. 3, Chapter 7.
(21) Cohen, C., submitted for publication.
(22) (a) Wales, J. L. S.; Philippoff, W. *Rheol. Acta* **1973**, *12*, 25. (b) Osaki, K.; Bessho, N.; Kojimoto, T.; Kurata, M. *J. Rheol.* **1979**, *23*, 457. (c) Gortemaker, F. H.; Hansen, M. G.; deCindio, B.; Janeschitz-Kriegl, H. *Rheol. Acta* **1976**, *15*, 242.